Obtaining optimal structural data from X-ray powder diffraction using the Rietveld method

Shanke Liu[1,a] He Li,[2] and Jianming Liu[1]
[1]*Division of Solid Mineral Resources, Institute of Geology and Geophysics, Chinese Academy of Sciences, Beijing 100029, China*
[2]*State Key Laboratory of Lithospheric Evolution, Institute of Geology and Geophysics, Chinese Academy of Sciences, Beijing 100029, China*

(Received 1 April 2014; accepted 11 July 2014)

Diffraction data of calcite were collected using a conventional Bragg–Brentano diffractometer, which is a convenient, low-cost, and highly popular in-house instrument, and its crystal structure was refined by the Rietveld method. This paper shows how one treats preferred orientation and how different refinement strategies affect the accuracy of the result. © *2014 International Centre for Diffraction Data*. [doi:10.1017/S0885715614000682]

Key words: calcite, crystal structure, refinement strategy, preferred orientation

I. INTRODUCTION

X-ray powder diffraction (XRPD) is a widely used method used for phase identification and quantitative analysis. Significant progress in powder methods occurred in the 1970s after Hugo Rietveld introduced a powerful technique for refining crystal structures from powder data in 1967 (Rietveld, 1967).

How to acquire good-quality powder diffraction data and how to refine using appropriate strategies have been stressed by many experts in order to extract good-quality structural data (Hill, 1992; Young, 1993; Hill and Cranswick, 1994; McCusker *et al.*, 1999; Toby, 2006; Kaduk, 2009). Experienced users of the Rietveld method are probably familiar with most requirements for obtaining good-quality structural data. However, novices will benefit from repetition of some key points, which are reviewed here using some examples. We report here Rietveld refinements of calcite – a well-known structure that has been successfully refined many times (Markgraf and Reeder, 1985; Antao *et al.*, 2009; Ballirano, 2011). Calcite exhibits rhombohedral cleavage and its powder commonly has a preferred orientation when loaded into a flat-plate sample holder. When the preferred orientation is unavoidable, using a proper model is an important but not difficult matter, as the expected results are known. We can thus test the impact of different preferred orientation models on structural parameters. Herein, we show how one treats preferred orientation and how one chooses the appropriate refinement strategies.

II. SAMPLES AND MEASUREMENT

A. Samples

Two calcite samples were used: one was from Mishan, Heilongjiang Province, China (Mishan, containing small amounts of impurities), and the other was from Rock-Mineral Preparation and Analysis Lab at the Institute of Geology and Geophysics, Chinese Academy of Sciences (IGGCAS). The second sample is labeled as Occ (Single phase).

B. Acquisition of XRPD patterns

Each sample was uniformly ground using a mortar and pestle and passed through a 200-mesh sieve. Step-scanned patterns were acquired using a Rigaku D/max–2400 Bragg–Brentano diffractometer fitted with a graphite diffracted-beam monochromator (Rigaku Corporation, Japan). Given that calcite tends to orient strongly, the samples were prepared by the backloading method to reduce the effects of the preferred orientation. Details are presented in Table I. The Mishan sample contains few impurities (clinochlore and quartz); therefore, a quantitative phase analysis was performed on several coexisting phases during structural refinements.

III. THE RIETVELD REFINEMENT

The Rietveld method, which was initially proposed by Rietveld (1967, 1969), has been significantly improved during the past two decades and has become an effective, reliable tool for the structural refinements.

TABLE I. XRD pattern measurement conditions.

Instrument	Rigaku Dmax2400
Radiation	Cu-anode tube, operated at 40 kV and 100 mA
	Wavelength: Cu$K\alpha$ = 1.5418 Å, Cu$K\alpha_1$ = 1.540 60 Å, and Cu$K\alpha_2$ = 1.544 39 Å
Optics	Bragg–Brentano
	Divergence slit = 1°, scatter slit = 1°, and receiving slit = 0.15 mm
Specimen	holder: rectangular aluminum plates with a rectangular window
Detection	Graphite-diffracted beam monochromator set for Cu$K\alpha$
	NaI scintillator detector
Acquisition	Angular range in 2θ: 3°–140° for Mishan, 15°–140° for Occ
	Step size: 0.02°
	Counting time: 0.5 s step^{-1}

[a]Author to whom correspondence should be addressed. Electronic mail: liushanke@mail.iggcas.ac.cn

https://doi.org/10.1017/S0885715614000682 Published online by Cambridge University Press

The free online computer program package General Structure Analysis System (GSAS) (Larson and Von Dreele, 2000) and a graphical interface for the GSAS package (EXPGUI) (Toby, 2001) were used for the structural refinements. The quality of agreement between the experimental and calculated profiles obtained from the programs was verified using the LaB_6 standard (SRM 660b, National Institute of Standards and Technology) XRPD pattern. The instrumental parameter file was obtained from the profile terms from the LaB_6 fit. The initial atomic coordinates, cell parameters, isotropic temperature factors (which were recast using the formula $U_{iso} = B_{iso}/8\pi^2$ for comparison to older literature values), and space group for calcite, clinochlore, and quartz were obtained from Markgraf and Reeder (1985), Walker and Bish (1992), and Lager *et al.* (1982), respectively.

A. Occ refinement

A full-matrix, least-squares refinement was carried out using the following process for adding parameters. First, the scale factor was refined, and then the background was modeled using a two-term shifted Chebyshev polynomial [Figure 1(a)]. The initial refinement yielded the residuals $R_{wp} = 49.3$ and $\chi^2 = 20.7$. It was obvious from looking at a plot of the observed and computed patterns that the background needed more terms to further improve the fit. The residuals dropped to $R_{wp} = 26.1$ and $\chi^2 = 5.81$ after the background was modeled using a four-term Chebyshev polynomial [Figure 1(b)].

From Figure 1(b), we can see that the differences between the observed and calculated patterns are very obvious, and this is mainly caused by the preferred orientation. The third CW profile function was used to describe the diffraction peaks. The diffractometer zero was verified to be close to zero in the refinement from the standard and in any case should not be refined under normal circumstances with Bragg–Brentano datasets. Instead, only the specimen displacement coefficient (*shft* in GSAS) was refined. Next, based on these values in the instrument file, the *U*, *V*, and *W* (Cagliotti) terms were modified separately, and they were fixed in the following cycles. Note that in this example, these instrumental terms were not determined from a standard. If they had been, a better procedure would be to leave these values fixed and only refine the crystallite size broadening term, *P*. Additionally, the profile coefficient *Y*, which describes the microstrain broadening, was also added. Refinement of these ten variables yielded the residuals $R_{wp} = 25.7$ and $\chi^2 = 5.65$. The *R* factors show that the improvements are not large. Then, the cell parameters were added to the refinement in the following step, and the fit plot [Figure 1(c)] showed that the description of the background needed improvement. Therefore, additional Chebyshev polynomial terms were added one-by-one, until no significant additional improvement was seen, when ten terms were introduced. Then, the fit of background further improves [Figure 1(d)], and the residuals for refinement of 18 variables dropped considerably: $R_{wp} = 23.6$ and $\chi^2 = 4.75$.

These data clearly exhibit strong preferred orientation, so these refinements provide a good test case to illustrate how

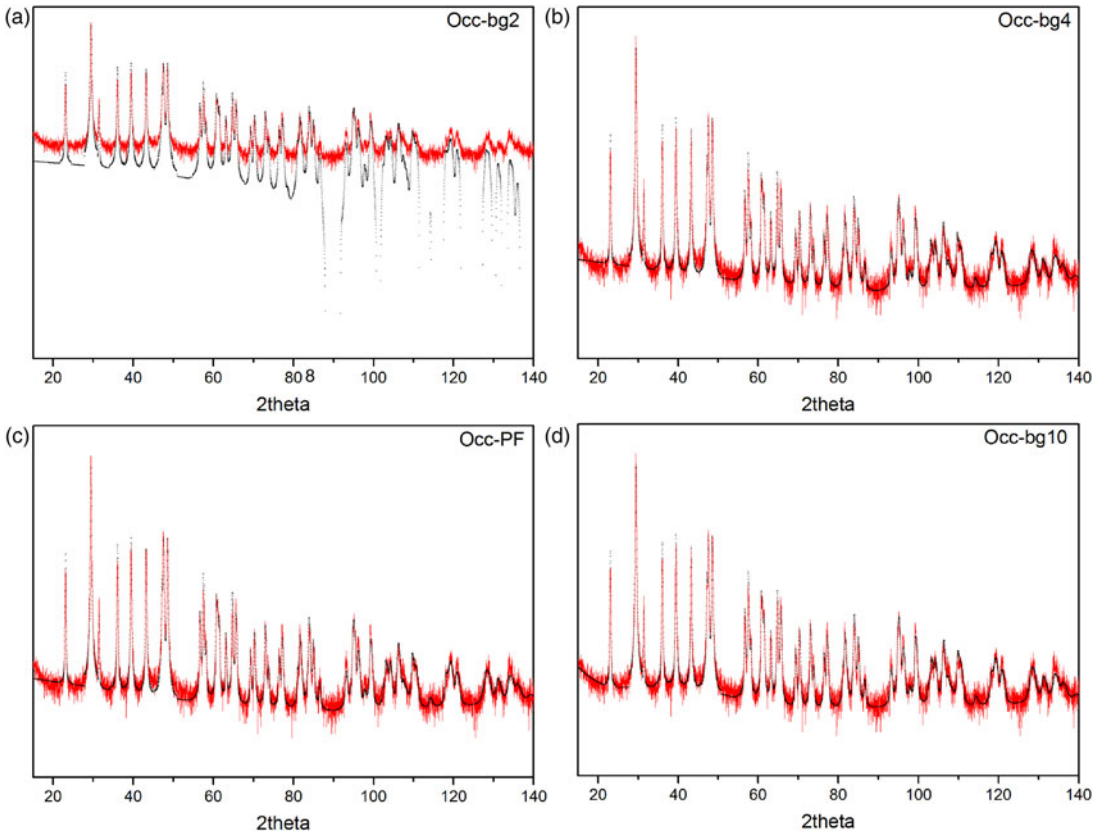


Figure 1. (Color online) Rietveld fit of Occ when a two terms Chebyshev polynomial, a four terms Chebyshev polynomial, profile and cell parameters and a ten terms Chebyshev polynomial were added to the refinement, respectively, and the corresponding plots are Figures 1(a)–1(d) (the log vertical scale was chosen for clarity). The red curve is observed diffraction pattern (line), and the black is calculated (crosses).

https://doi.org/10.1017/S0885715614000682 Published online by Cambridge University Press

treatments for this affects the accuracy of the structural data through comparison of four different refinement strategies.

In the first approach, no treatments for the preferred orientation were added prior to inclusion of the structural parameters (this model including no March-Dollase function is labeled NMD). Addition of the positional and isotropic temperature parameters to the refinement resulted in residuals dropping to: $R_{wp} = 21.9$ and $\chi^2 = 4.11$ (Figure 2).

In the second method, the preferred orientation was modeled by the March–Dollase (MD) function. Based on the trial-and-error method, the preferred orientation can be easily recognized on powder diffraction photographs if one type of the preferred orientation is present. However, if more than one type of the preferred orientation is present, this approach is almost useless. By calculating the Bravais–Friedel–Donnay–Harker crystal morphology (Bravais, 1866; Friedel, 1907; Donnay and Harker, 1937), we know the growth direction of calcite is complex (Figure 3), and the texture is also complex for natural calcite (Wenk and Houtte, 2004). Figure 2 shows the cumulative χ^2, which can be expected to rise with a constant slope of unity, but with a much more steep increase in regions of the pattern that are poorly fit. The cumulative χ^2 for the NMD refinement shows a large mismatch for the *104* diffraction peak, and *104* is also one of the growth directions of the calcite crystal; therefore the *104* direction was chosen as the preferred orientation axis in a refinement labeled as MD1. This resulted in greatly improved residuals, $R_{wp} = 15.5$ and $\chi^2 = 2.04$. However, the natural calcite rocks often exhibit a strong preferred orientation along the *c*-axis (Wenk and Houtte, 2004), which is not inconsistent with *006* as one of the growth directions of the calcite crystal (Figure 3), and this can be noted from the large mismatch in the cumulative χ^2 for the *006* diffraction peak in Figure 2. Therefore, a refinement with *001* instead of *104* MD preferential orientation direction was performed as MD2 obtaining residuals, $R_{wp} = 17.4$ and $\chi^2 = 2.58$.

Several researchers (Sitepu, 2002; Sitepu *et al.*, 2005; Balic-Zunic *et al.*, 2011) have shown that the spherical harmonics function (SPH) is superior to the MD function in terms of

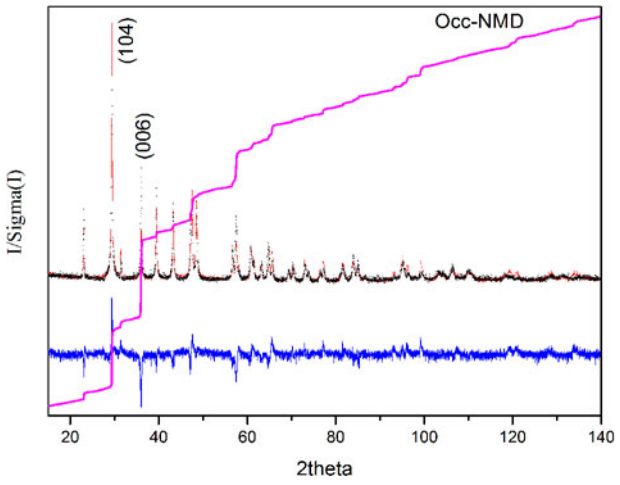


Figure 2. (Color online) Rietveld fit of Occ–NMD: the red curve is observed diffraction pattern (line), and the black is calculated (crosses); vertical marks indicate the positions of allowed $K\alpha_1$ and $K\alpha_2$ reflections; the blue curve at the bottom shows the difference between observed and calculated patterns (line); the pink curve is cumulative χ^2 (line).

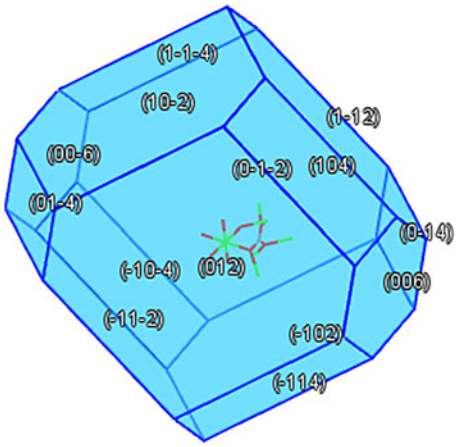


Figure 3. (Color online) Bravais–Friedel–Donnay–Harker crystal morphology of calcite.

modeling the preferred orientation effects. Therefore, SPH was used to correct the peak intensities, and two harmonic orders were chosen at the beginning. The harmonic orders were gradually increased until the *R* factors did not further decrease. Last, ten harmonic orders were chosen, and this is consistent with the report of Sitepu *et al.* (2005). Compared with the residuals of MD1 and MD2, the residuals dropped to $R_{wp} = 13.5$ and $\chi^2 = 1.56$.

The position and isotropic temperature parameters were varied after the preferred orientations treatments were incorporated for the MD1, MD2, and SPH models. The details of the refined crystal structural parameters obtained from different refinement strategies are given in Table II.

B. Mishan refinement

The same strategy was applied to refine the Mishan sample. However, besides the major phase calcite (98.21%), Mishan contains two minor impurity phases, quartz (0.40%) and clinochlore (1.39%). These impurity phases (since their amounts are quite small) have only a minor impact on the overall refinement. Accordingly, only their individual cell and phase fraction parameters were optimized during the refinement. The profile parameters of these two minor phases were approximated by constraining them to be the same as those of the major calcite phase. Compared with Occ, a similar trend was found when the preferred orientation was modeled for the calcite phase of Mishan through MD1, MD2, and SPH, respectively, but only the latter result is presented. These data have greater preferred orientation, as noted by the texture index. If the texture index is equal to one, it means random texture; if it is close to three, it means a strong texture. When it is higher than three, the diffraction data may be over fitted.

In carbonates, the expected C–O bond length is 1.28–1.29 Å based on single-crystal X-ray diffraction (SC-XRD) (Effenberger *et al.*, 1981; Reeder and Wenk, 1983; Markgraf and Reeder, 1985; Zucchini *et al.*, 2012), synchrotron X-ray powder diffraction (SN-XRPD) (Antao *et al.*, 2009), and parallel-beam transmission X-ray powder diffraction (PT-XRPD) (Ballirano, 2011) data. However, for the Mishan sample, in the SPH fit the C–O bond length of

https://doi.org/10.1017/S0885715614000682 Published online by Cambridge University Press

TABLE II. Details of the refined crystal structure parameters of two calcite samples.

		Occ				Calcite of Mishan		
		NMD	MD1	MD2	SPH	SPH	SDC-1	SDC-2
Cell	a (Å)	4.9834(1)	4.9863(2)	4.9839(1)	4.9866(2)	4.986 73(5)	4.986 75(5)	4.986 76(5)
parameters	c (Å)	17.0650(7)	17.0799(8)	17.0678(4)	17.0816(7)	17.0510(2)	17.0506(2)	17.0506(2)
	V (Å^3)	367.02(2)	367.77(4)	367.16(2)	367.84(4)	367.207(9)	367.203(9)	367.204(9)
Atom site	x_O	0.2485(4)	0.2542(3)	0.2506(3)	0.2572(5)	0.2529(4)	0.2555(2)	0.257 33(8)
Biso	Ca	1.69(4)	0.97(2)	1.48(3)	1.03(3)	1.32(3)	1.31(3)	1.33(3)
	C	1.68(4)	0.96(2)	1.47(3)	1.02(3)	0.97(10)	0.95(10)	1.02(10)
	O	2.26(4)	1.54(2)	2.05(3)	1.60(3)	1.72(6)	1.70(6)	1.70(6)
Bong length	Ca–O	2.380(1)	2.3663(9)	2.3743(9)	2.359(1)	2.368(1)	2.3617(6)	2.3571(2)
	C–O	1.238(2)	1.268(1)	1.249(1)	1.283(3)	1.261(2)	1.274(1)	1.2832(4)
Bond valence	Ca	1.967(2)	2.039(2)	1.995(2)	2.080(3)	2.072(3)	2.064(1)	2.091(1)
Sums	C	4.519(10)	4.177(7)	4.392(7)	4.011(11)	4.250(9)	4.103(5)	4.003(2)
	O	2.162(8)	2.072(6)	2.129(6)	2.030(9)	2.092(8)	2.056(4)	2.031(1)
R factors	R_{WP}	21.9	14.4	16.2	12.6	14.8	14.7	14.9
	R_P	17.4	10.4	12.9	8.58	10.6	10.3	10.5
	R_{exp}	10.8	10.8	10.8	10.8	9.79	9.79	9.79
	R_F^2	19.7	10.5	11.0	4.76	13.8	13.5	14.2
	χ^2	4.11	1.78	2.23	1.36	2.29	2.23	2.31
W_{SDC}(%)		/	/	/	/	/	1.59	0.40
Restraint weight		/	/	/	/	/	50	500
Texture index		/	/	/	1.41	2.18	2.21	2.25

Note: 1. NMD denotes a model without preferred orientation treatments. MD1 denotes that only the preferred parameters along the 104 direction are refined through the March–Dollase model. MD2 denotes that the preferred parameters along the 001 axe are both refined through the MD model. SPH denotes that the SPH is introduced into the structural model to treat the preferred orientation. SDC-1 denotes that the restraint weight is set as 50 for the C–O bond length restraint and SDC-2 denotes that the restraint weight is 500.
2. Standard uncertainties are given in parentheses.

calcite is about 1.26 Å, significantly shorter than what is expected. This is likely because of the correlation between the spherical harmonic and crystallographic parameters producing a range of models that provide very similar fits. To provide the most credible result, a restraint was introduced on the distance between the C and O atoms for the calcite phase of Mishan. The target value and uncertainty for the restraint were set as 1.285 ± 0.01 Å, and refinements with two different restraint weights, 50 (SDC-1) and 500 (SDC-2), were performed. These refinements produced minor changes in the overall fit with: $R_{wp} = 14.8$, 14.7, and 14.9 and $\chi^2 = 2.29$, 2.23, and 2.31 for SPH, SDC-1, and SDC-2, respectively. The contribution of the distance restraint to the overall refinement (W_{SDC}) is minor, with a contribution to the χ^2 of 1.59 and 0.40%, respectively, for SDC-1 and SDC-2. Note that as the restraint weight is increased, both the bond length and texture index increase, but W_{SDC} decreases. In this paper, it is not a key point that the authors discuss the relation between W_{SDC} with the restraint weight, only a reference paper published by Nowell *et al.* (2002) is recommended.

From a chemical point, an appropriate weight of the distance restraint is indispensable to obtain a reasonable bond length for the Mishan sample. However, the correlation among refined parameters should be checked. Therefore, the correlation matrix were output by clicking on "Print the correlation matrix" in the LS controls menu. The authors found that the correlation among refined parameters for SPH, SDC-1, and SDC-2 fits are very similar, and so only the correlation coefficients of SDC-2 as an example are shown:

From the above correlation matrix terms, we can see that the background parameters correlate highly among each other, which is common for Chebyschev polynomial terms. This is also true for the spherical harmonic terms. Note that the background and spherical harmonic terms do not correlate with other parameters to a significant degree. This demonstrates the relative insensitivity to the combination of these parameters. The Uiso thermal parameters of Ca and O atoms

```
The correlation matrix terms greater than 0.50 are
1  1UISO-1  1PHFR   697
1  3UISO-1  1PHFR   503
1   RM11-1  1PF10   681
1   RM33-1  1PF10   652
2   RM11-2   RM33  -829
1  OD001-1  OD008  -665
1  OD002-1  OD005  -531
1  OD004-1  OD008   616
1  OD005-1  OD007   510
1  1PF 1-1  1PF 6  -738
   1BK 1-   1BK 2  -719   1BK 3   846   1BK 4  -675   1BK 5   740   1BK 6  -578   1BK 7   585
   1BK 2-   1BK 3  -755   1BK 4   857   1BK 5  -684   1BK 6   729   1BK 7  -539   1BK 8   535
   1BK 3-   1BK 4  -745   1BK 5   850   1BK 6  -633   1BK 7   662
   1BK 4-   1BK 5  -724   1BK 6   820   1BK 7  -594   1BK 8   636
   1BK 5-   1BK 6  -693   1BK 7   781   1BK 8  -531   1BK 9   545
   1BK 6-   1BK 7  -640   1BK 8   766
   1BK 7-   1BK 8  -586   1BK 9   663
   1BK 8-   1BK 9  -500   1BK10   640
v-cov distribution 0...1 by 0.05
   583   39   19   11    9    6    7   15    8    4    8    4    5    9    6    3    4    1    0    0
```


https://doi.org/10.1017/S0885715614000682 Published online by Cambridge University Press

TABLE III. Details of the published structure parameters of calcite.

		Markgraf and Reeder	Antao *et al.*	Sitepu *et al.*[a]	Ballirano[a]
Cell	a (Å)	4.988(1)	4.987 7648(1)	4.9920(5)	4.988 79(7)
Parameters	c (Å)	17.061(1)	17.052 42(2)	17.069(2)	17.0649(4)
	V (Å^3)	367.6(1)	367.3911(4)	368.3731	367.81(1)
Atom sites	x_O	0.2567(2)	0.257 34(6)	0.250(1)	0.2564(9)
B_{iso}	Ca	0.94(3)	0.80(4)	1.203(4)	–
	C	0.93(5)	0.76(6)	1.644(2)	–
	O	1.51(4)	1.44(6)	1.644(2)	–
Bond	Ca–O	2.3595(5)	2.3574(2)	2.379(1)	2.3608(7)
Length	C–O	1.280(1)	1.2836(3)	1.248(2)	1.279(1)
Method		SC-XRD	SN-XRPD	BB-XRPD	PB-XRPD

Note: [a]Bond lengths are calculated in terms of cell parameters and atomic coordinates in their studies. Standard deviations are given in parentheses.

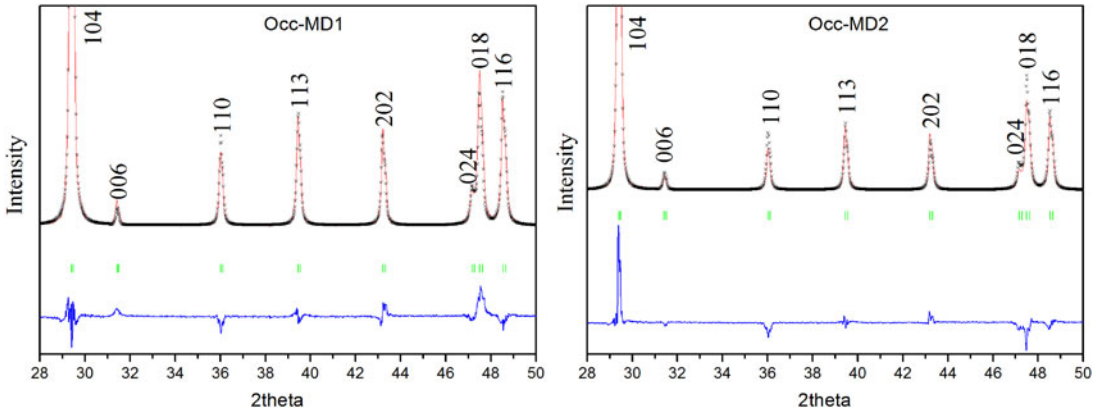


Figure 4. (Color online) Enlargement of Rietveld fit of Occ–MD1 (a) and Occ–MD2 (b), respectively: the red curve is observed diffraction pattern (line), and the black is calculated (crosses); vertical marks indicate the positions of allowed $K\alpha_1$ and $K\alpha_2$ reflections; the blue curve at the bottom shows the difference between observed and calculated patterns (line).

are closely correlated with the weight fraction of calcite phase, which shows that careful consideration of the Uiso values is necessary if the most accurate quantitative analyses are to be obtained. Correlation values in the range of 0.5–0.75 are rarely problematic in Rietveld fits and even values up to 0.95 usually refine well, perhaps with need for some damping on shifts. Here, most values are less than 0.75 and none are above 0.9.

IV. RESULTS AND DISCUSSION

The published structural parameters of calcite (Markgraf and Reeder, 1985; Sitepu *et al.*, 2005; Antao *et al.*, 2009; Ballirano, 2011) are also provided in Table III for comparison with the data in Table II. The Rietveld fits of Occ are shown in Figures 4 and 5 using different treatments to model the preferred orientation, and the Rietveld fit of Mishan-SPH is shown in Figure 6. Cell parameters of Occ and calcite of Mishan are plotted against different refinement models in Figure 7. x_O sites of Occ and calcite of Mishan are also plotted against different refinement models in Figure 8.

A. *R* factors

1. Occ

Compared with these R factors obtained with no treatments for the preferred orientation, all R factors, significantly decrease when MD1, MD2, and SPH are introduced to model the preferred orientations (Table II). The significantly better fit obtained for SPH indicates it is superior to MD1 and MD2, and therefore the texture for these calcite data cannot be satisfactorily described by a single or two MD vectors (Figures 4 and 5).

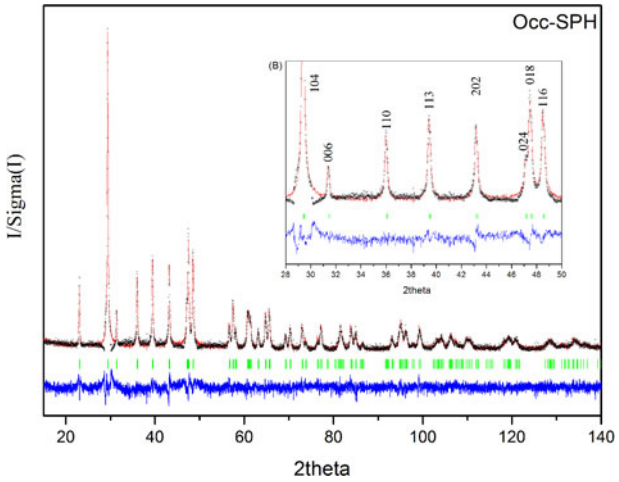


Figure 5. (Color online) (a) Rietveld fit of Occ–SPH: the red curve is observed diffraction pattern (line), and the black is calculated (crosses); vertical marks indicate the positions of allowed $K\alpha_1$ and $K\alpha_2$ reflections; the blue curve at the bottom shows the difference between observed and calculated patterns (line). (b, inset) Enlargement of Rietveld fit of Occ–SPH.

https://doi.org/10.1017/S0885715614000682 Published online by Cambridge University Press

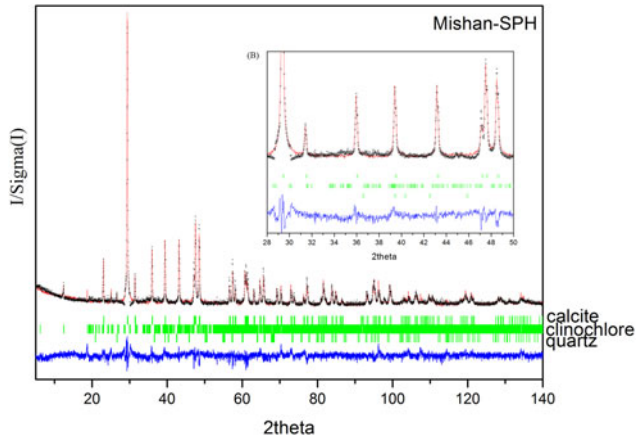


Figure 6. (Color online) (a) Rietveld fit of Mishan–SPH: the red curve is observed diffraction pattern (line), and the black is calculated (crosses); vertical marks indicate the positions of allowed $K\alpha_1$ and $K\alpha_2$ reflections; the blue curve at the bottom shows the difference between observed and calculated patterns (line). (b, inset) Enlargement of Rietveld fit of Mishan–SPH.

2. Mishan

When a restraint is added to the model, the *R* factors slightly change (Table II). All of three fits are visually indistinguishable. Toby (2006) stated that agreement factors are not the only indicators of the quality of a Rietveld fit and the greater chemical plausibility allows us to state that model SDC-2 is preferred.

B. Cell parameters

The standard uncertainties (ESDs) in this paper are larger than those values obtained from SN-XRPD (Antao *et al.*, 2009), but they are smaller than those values from SC-XRD (Markgraf and Reeder, 1985) (Figure 7, Tables II and III). The improved precision of synchrotron data is to be expected, but shows that laboratory powder diffraction can be competitive or better than single-crystal measurements of cell dimensions. A search in the PDF-4+ 2013 (published by ICDD) for star quality, ambient, Ca/C/O only, and space group #167 yielded 11 PDF cards. The average lattice parameters of cells a and c were 4.989(3) and 17.062(13) Å, respectively, and were added into the corresponding pictures in Figure 7 as a reference (Star in Figure 7). It is very obvious that the calcite cell parameters obtained through different models approach basically the coverage of the average lattice parameters of 11 PDF cards. In general, the cell parameters of calcite are closely related to its composition. Then, a further search in the PDF-4+ 2013 (published by ICDD) for star quality, ambient, magnesium calcium carbonate, and space group #167 yielded seven hits. Three of them were chosen that visually agreed well with our measurement, and the parameters

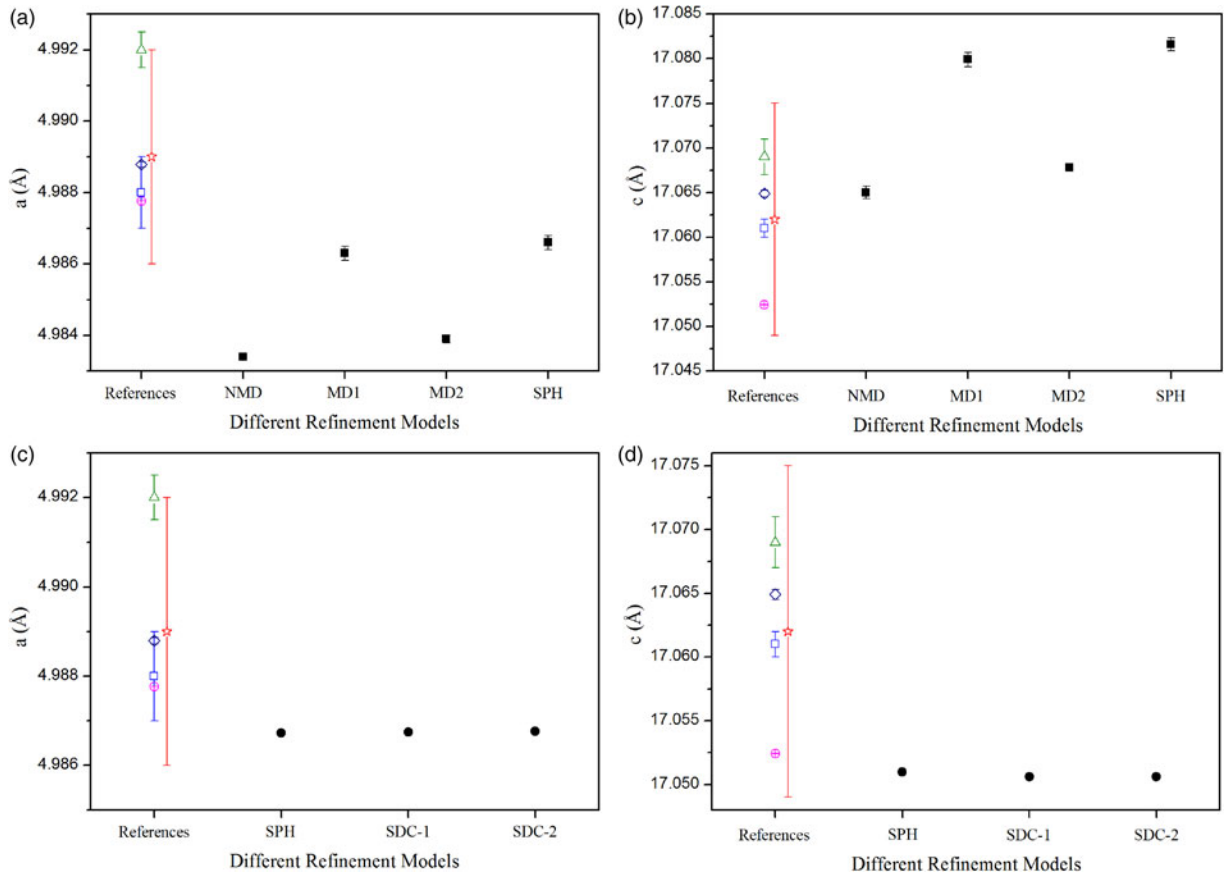


Figure 7. (Color online) Cell parameters of Occ and calcite phase of the Mishan sample plotted against different refinement models (DRM): (a) *a* of Occ versus DRM; (b) *c* of Occ versus DRM; (c) *a* of calcite of Mishan versus DRM; (d) *c* of calcite of Mishan versus DRM. ■ Occ; ● Calcite of Mishan; □ Mark graf and Reeder; ○ Antao *et al.*; △ Sitepu *et al.*; ◇ Ballirano; ★ the average lattice parameters of 11 PDF cards. The vertical bars represent errors. If no bar is given, then the error is contained within the area of the symbol.

https://doi.org/10.1017/S0885715614000682 Published online by Cambridge University Press

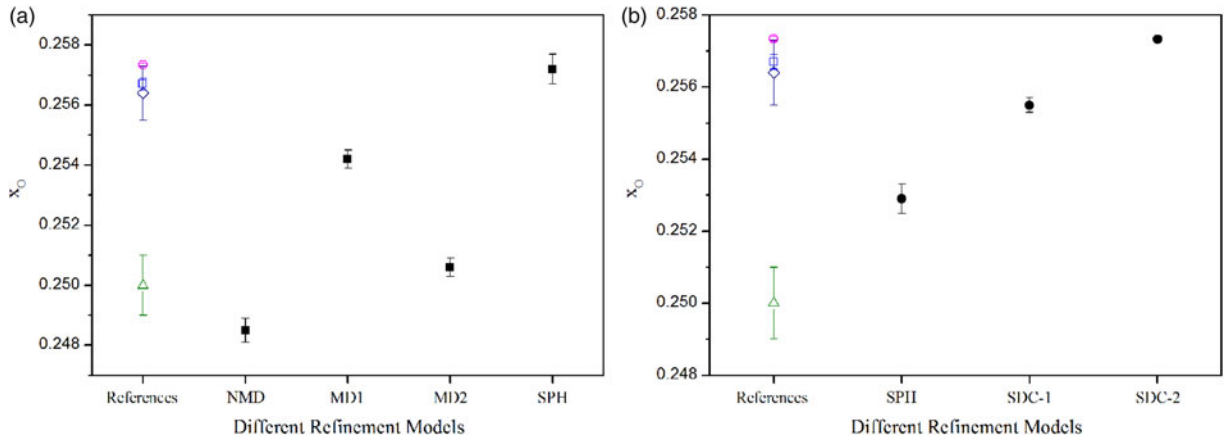


Figure 8. (Color online) x_O sites plotted against different refinement models (DRM): (a) Occ; (b) calcite phase of the Mishan sample. ■ Occ; ● Calcite of Mishan; □ Mark graf and Reeder; ○ Antao *et al.*; △ Sitepu *et al.*; ◇ Ballirano. The vertical bars represent errors. If no bar is given, then the error is contained within the area of the symbol.

cell a from three PDF cards (01-086-2336, 01-089-1304, and 01-089-1305) were plotted against the Ca atoms in the chemical formula in Figure 9. A linear fit was analyzed for three sets of figures, and a linear equation $y = 4.6119 + 0.3745x$ ($R = 0.9983$) was obtained. Both Ca atom numbers in the chemical formula calculated by the linear equation are little larger than 1 for Occ and the calcite phase of Mishan. Although it is a rough calculation, this still shows that the cell parameters refined from powder diffraction in this paper agree with these published ones very well.

1. Occ

Compared with those from MD1 and SPH, the cell parameters from NMD and MD2 are clearly smaller (approximately tens of σ) [Table II and Figures 7(a) and 7(b)] showing that untreated or improper preferred orientation can skew these parameters. However, the cell parameters show negligible changes (approximately few σ) when MD1 and SPH are applied to modify the preferred orientation, and agree well with the literature, as shown in Figures 7(a) and 7(b).

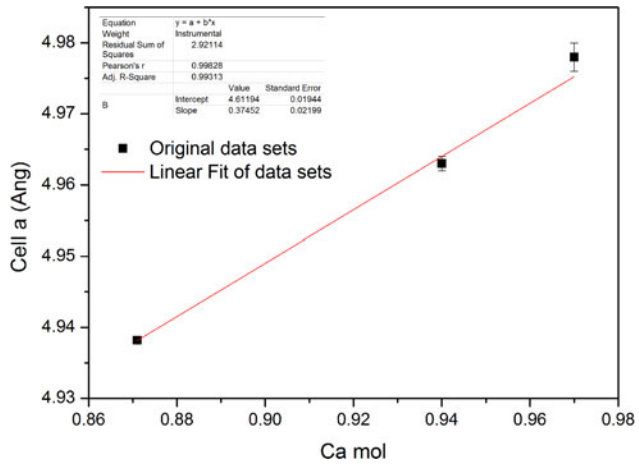


Figure 9. (Color online) Cell a of three PDF cards plotted against Ca mol for calcite, and a linear fit was analyzed.

2. Calcite of Mishan

The cell parameters of calcite of Mishan also approach the literature values obtained by Antao *et al.* (2009) when SPH, SDC-1, and SDC-2 are applied [Figures 7(c) and 7(d)]. Compared with these values from SPH, the cell parameters of calcite of Mishan are nearly unchanged when SDC is further applied, and the changes are approximately ± 1 σ [Tables II and III, Figures 7(c) and 7(d)].

C. Isotropic displacement factors

The different refinement models show negligible effects on the isotropic displacement factors. Even without treatment for preferred orientation in the NMD model, the Uiso values are still quite reasonable. Similarly, a search in the PDF-4+ 2013 (published by ICDD) for star quality, ambient, calcite, and space group #167 yielded 18 PDF cards, but only three PDF cards (04-012-6929, 04-012-6930, and 04-013-2116) provide the Biso or Uiso values. The isotropic displacement factors in this paper are in accord with these values in the three PDF cards.

D. Bond lengths, atomic coordinates, and bond valence sums

Tables II and III show that the incorporation of preferred orientation treatments brings the Ca–O and C–O bond lengths much closer to the consensus literature values, and likewise for the atomic coordinate x_O (Figure 8). Note that since the model has only one refinable structural parameter, x_O, this value and the lattice parameters determine the interatomic distances. ESD values from the SPH model are slightly larger than those reported by Antao *et al.* (2009) and Markgraf and Reeder (1985).

With different refinement models, the changes of bond valence sums of Ca, C, and O atoms calculated by the program Bond_Str (Brown and Altermatt, 1985; Brown, 2002) are in accord with the ones of the bond lengths (Table II), and it is reasonable because the bond sums are closely related to the bond lengths. As a result, the bond sums are closer to the theoretical values when the C–O bond length approaches 1.28 Å.

https://doi.org/10.1017/S0885715614000682 Published online by Cambridge University Press

E. Reasons why different refinement models have different effects on the structural data and the credibility of the structural data

The introduction of preferred orientation models, whether modeled by MD or SPH, makes a significant impact on the resulting structural data, including the cell parameters, the bond lengths, and the atomic coordinates. However, after MD or SPH functions are introduced, preferred orientation treatments are correlated with the bond lengths and atomic coordinates, but not with the cell parameters. This can be understood because a preferred orientation affects the peak intensities, but not the peak positions. The cell parameters depend on the peak positions, whereas the atomic coordinates depend on the peak intensities. The preferred orientation models change the calculated structural factors and thus affect the atomic coordinates.

The bond lengths of calcite are consistent with the values obtained from the refinement of SC-XRD (Markgraf and Reeder, 1985), SN-XRPD (Antao *et al.*, 2009), and PT-XRPD (Ballirano, 2011) data for Occ. However, in the more highly textured Mishan sample, accurate bond lengths were not obtained until a restraint on distances was introduced. If one is using Rietveld analysis to determine bond distances, it is clear that significant levels of texture may introduce problems.

In summary, we conclude that the preferred orientation is the principal factor that affects the quality of the BB-XRPD diffraction data for calcite.

ACKNOWLEDGEMENTS

The authors acknowledge the financial support for technological innovations from the Institute of Geology and Geophysics, Chinese Academy of Sciences. Shanke Liu is indebted to Professor Jiaju Li for his tremendous help and encouragement in studying the Rietveld method. Shanke Liu is also grateful to Dr. B.H. Toby for helping with GSAS refinement skills and tremendous encouragement in preparing this paper through private communications. Two anonymous reviewers are thanked for their constructive critical suggestions aimed to improve the quality of the manuscript.

SUPPLEMENTARY MATERIALS AND METHODS

The supplementary material for this article can be found at http://www.journals.cambridge.org/pdj.

Antao, S. M., Hassan, I., Mulder, W. H., Lee, P. L., and Toby, B. H. (**2009**). "*In situ* study of the R-3c → R-3m orientational disorder in calcite," Phys. Chem. Miner. **36**, 159–169.

Balic-Zunic, T., Katerinopoulou, A., and Edsberg, A. (**2011**). "Application of powder X-ray diffraction and the Rietveld method to the analysis of oxidation processes and products in sulphidic mine tailings," Neues Jahrb. Miner. Abh. **188**(1), 31–47.

Ballirano, P. (**2011**). "Laboratory parallel-beam transmission X-ray powder diffraction investigation of the thermal behavior of calcite: comparison with X-ray single-crystal and synchrotron powder diffraction data," Period Miner. **80**(1), 123–134.

Bravais, A. (**1866**). *Etudes Cristallographiques* (Gauthier-Villars, Paris), pp. 1811–1863.

Brown, I. D. (**2002**). "The chemical bond in inorganic chemistry: the bond valence model," in *IUCrMonographs on Crystallography*, 12 (Oxford University Press, New York, NY).

Brown, I. D. and Altermatt, D. (**1985**). "Bond-valence parameters obtained from a systematic analysis of the inorganic crystal structure database" Acta Crystallogr. **B41**, 244–247.

Donnay, J. D. H. and Harker, D. (**1937**). "A new law of crystal morphology extending the Law of Bravais," Am. Miner. **22**, 463–467.

Effenberger, H., Mereiter, K., and Zemann, J. (**1981**). "Crystal structure refinements of magnesite calcite, rhodochrosite siderite, smithonite and dolomite, with discussion of some aspects of the stereochemistry of calcite type carbonates," Z. Kristallogr. **156**, 233–243.

Friedel, G. (**1907**). "Studies on the law of Bravais," Bull. Soc. Franc. Miner. **30**, 326–455.

Hill, R. J. (**1992**). "Rietveld refinement round robin. I. Analysis of standard X-ray and neutron data for $PbSO_4$," J. Appl. Crystallogr. **25**, 589–610.

Hill, R. J. and Cranswick, L. M. D. (**1994**)."International union of crystallography commission on powder diffraction Rietveld refinement round robin. II. Analysis of monoclinic ZrO_2," J. Appl. Crystallogr. **27**, 802–844.

Kaduk, J. A. (**2009**). "A Rietveld Tutorial – Mullite," Powder Diffr. **24**(4), 351–361.

Lager, G. A., Jorgensen, J. D., and Rotella, F. J. (**1982**). "Crystal structure and thermal expansion of alpha-quartz SiO_2 at low temperatures," J. Appl. Phys. **53**, 6751–6756.

Larson, A. C. and Von Dreele, R. B. (**2000**). *General Structure Analysis System (GSAS)* Los Alamos National Laboratory Report. LAUR, pp. 86–748.

Markgraf, S. A. and Reeder, R. J. (**1985**). "High-temperature structure refinements of calcite and magnesite" Am. Miner. **70**, 590–600.

McCusker, L. B., Von Dreele, R. B., Cox, D. E., Louër, D., and Scardi, P. (**1999**). "Rietveld refinement guidelines," J. Appl. Crystallogr. **32**, 36–50.

Nowell, H., Attfield, J. P., and Coleb, J. C. (**2002**). "The use of restraints in Rietveld refinement of molecular compounds; a case study using the crystal structure determination of tryptamine free base," Acta Crystallogr. **B58**, 835–840.

Reeder, R. J. and Wenk, H. R. (**1983**). "Structure refinements of some thermally disordered dolomites," Am. Miner. **68**, 769–777.

Rietveld, H. (**1967**). "Line profiles of neutron powder-diffraction peaks for structure refinement," Acta Crystallogr. **22**, 151–152.

Rietveld, H. (**1969**). "A profile refinement method for nuclear and magnetic structures," J. Appl. Crystallogr. **2**, 65–71.

Sitepu, H. (**2002**). "Assessment of preferred orientation with neutron powder diffraction data," J. Appl. Crystallogr. **35**, 274–277.

Sitepu, H., O'Connor, B. H., and Li, D. (**2005**). "Comparative evaluation of the March and generalized spherical harmonic preferred orientation models using X-ray diffraction data for molybdite and calcite powders," J. Appl. Crystallogr. **38**, 158–167.

Toby, B. H. (**2001**). "EXPGUI, a graphical user interface for GSAS," J. Appl. Crystallogr. **34**, 210–213.

Toby, B. H. (**2006**). "R factors in Rietveld analysis: how good is good enough?," Powder Diffr. **21**(1), 67–70.

Walker, J. R. and Bish, D. L. (**1992**). "Application of Rietveld refinement techniques to a disordered IIb Mg-Chamosite," Clays Clay Miner. **40** (3),319–322.

Wenk, H. R. and Houtte, P. V. (**2004**). "Texture and anisotropy," Rep. Prog. Phys. **67**, 1367–1428.

Young, R. A. (**1993**). (Editor). *The Rietveld Method* (Oxford University Press, New York, NY).

Zucchini, A., Comodi, P., Katerinopoulou, A., Balic-Zunic, T., McCammon, C., and Frondini, F. (**2012**). "Order–disorder–reorder process in thermally treated dolomite samples: a combined powder and single-crystal X-ray diffraction study," Phys. Chem. Miner. **39**, 319–328.

https://doi.org/10.1017/S0885715614000682 Published online by Cambridge University Press